ATMOSPHERIC MODELLING FOR REALISTIC EDL SCENARIOS

Mark Paton[(1)], Walter Schmidt[(2)]

[(1)]Finnish Meteorological Institute, P.O. Box 503, Helsinki 00101, mark.paton@fmi.fi
[(2)]Finnish Meteorological Institute, P.O. Box 503, Helsinki 00101, walter.schmidt@fmi.fi

ABSTRACT

With manned flights planned to Mars during the next decades it becomes crucial to control the landing vehicles' entry, descent and landing as precisely as possible. All of the current scenarios foresee the deployment of an unmanned infrastructure before the manned landing takes place. A prerequisite for this approach is the possibility to constrain the area of touchdown of all mission vehicles to a manageable small area of only hundreds of meters in diameter. If large masses of fuel for navigating should be avoided, the atmospheric influences on the descent vehicles along the descent path have to be estimated as correctly as possible.

1. INTRODUCTION

Global models of the Martian atmosphere have been developed over the last decades and been compared with in-situ measurements from earlier and current Mars landing missions and with observations from orbiting remote sensing instruments. While they help to understand the development of large scale phenomena they are not detailed enough to provide the information about possible atmospheric influences on the descent trajectory of a landing vehicle. Based on meteorological high resolution weather forecast models used by the Finnish and other European meteorological institutes, we developed a 3D Mars Local Area Model (MLAM) to describe mesoscale developments of the Martian atmosphere [1]. Combining these results with boundary conditions used for the Aerobrake 2D program [2], high fidelity simulations for fine tuning EDLs are possible. Variations of temperature, atmospheric pressure and wind speed and direction as a function of altitude and ground topography can be used to optimize the entry scenario, shape of the entry vehicles and effective use of active guidance systems. A similar approach can be used for developing atmospheric reentry scenarios into the Earth atmosphere for sample return and manned missions. Different examples of such iterative optimization steps will be shown, based on vehicles described in the Mars for Less mission [3] and Apollo 6 reentry analysis [4].

2. MARS LOCAL-AREA MODEL

The Martian atmosphere is generally modelled using the same techniques as those used on Earth. General Circulation Models (GCM) for Mars provide global coverage and reproduction of large scale atmospheric phenomena. These models numerically solve fundamental thermal and mechanical equations for each atmospheric grid box. Typical resolutions of the grids are from 2 to 10°. For example the thermophysical GCM [5] has a typical resolution of 64 x 48 km or 5.5 x 3.25° and vertical coverage of 250 km with 60 layers. Established GCMs such as Ames GCM or the Oxford Mars GCM can operate over similar resolutions (e.g. see reference [6]). A GCM may operate with 2° grids for high spatial resolutions [7].

For higher grid resolutions and reproduction of small scale atmospheric phenomena nested models can be run over the area of interest using GCMs for boundary conditions. These types of simulation are referred to as mesoscale models and one example is the Mars Limited-Area Model (MLAM) developed at the University of Helsinki and the Finnish Meteorological Institute. A mesoscale model such as MLAM uses a grid that only covers a part of the globe, of say several thousand kilometres in size. A coarse grid simulation with MLAM may use 100 points over 100° whereas a fine grid simulation will use 200 points over 50° [1]. Mars has an equatorial radius of 3398 km so each degree is then about 60 km. A fine grid with 0.25° spacing then corresponds to a about a grid size of 15 km. The smallest grid size is dependant on the hydrostatic equation with the finest grids at 3-5 km [8]. The vertical grid is 32 levels and the atmosphere has its top at 48 km. The lowest level is at about 1.5 m. This level also corresponds to the level of the altitude at which Viking meteorological sensors were positioned [9]. The next level up is about 6.5 m. The levels are finely spaced near the surface and expand near the top of the atmosphere with a maximum spacing of 7 km at the top.

The layers in atmospheric models are defined using sigma coordinates. These are defined as the ratio of the pressure at a given point in the atmosphere to the pressure on the surface underneath it. This way a sigma level close to the surface will follow the terrain at approximately the same altitude. Sigma coordinates are used to simplify the lower boundary condition. Further

up in the atmosphere the levels become independent of the surface terrain. However with MLAM the sigma coordinates follow the terrain even at high altitude levels.

3. AEROBRAKE 2D

There are well tested high fidelity astrodynamical tools available for prototyping EDL systems for robotic mission to the planets (e.g. see reference [10]). These can model 6-degrees of freedom movement, simulate spacecraft thrusters and test guidance systems. However this level of sophistication is not required at the proof of concept stage for piloted landers as described in this type of work. A bare bones astrodynamical tool called Aerobrake 2D (A2D) has been developed evolving from fireball trajectory modelling work [2].

A2D simulates the motion of an object under the influence of gravitational and atmospheric drag forces. Newton's equation of motion is used, converted into 2D polar coordinates and expressed as four first order equations. The drag equation is used to model aerodynamic drag forces. Lift is simulated by adding a force perpendicular to the drag force and with a magnitude depending on a specified lift over drag (L/D) ratio. The simulation is coded in FORTRAN 77.

The first order equations of motion are iterated during each time step. For each discrete time step there is a step increase in the following, radial distance from the centre of the planet, radial velocity from the centre of the planet, angular distance around the planet, angular velocity around the planet. This approach is fairly accurate for a few orbits around a planet such as the Earth or Mars. For example a body orbiting the Earth starting at an altitude of 200 km, an initial speed of 7.9 m s^{-1} and a velocity vector angle of zero will increase its semi-major axis by 8 m each orbit when using a time step of 0.01 s. The program takes about 43 s to run that simulation. The error increases to ~km when using a time step of 0.1 s but the simulation takes only 5 s. Using a 0.1 s time step is certainly accurate enough for modelling a short path such as during aerocapture or EDL. Once a system has been defined the error due to numerical integration can easily be controlled using the time step with an error of around one metre at the end of the EDL path.

The atmosphere is modelled by dividing the atmosphere into sections bounded at specified altitude levels. For each level a temperature and wind speed are imported from the Mars Local-Area Model (MLAM), a mesoscale simulation of the Martian atmosphere or can be defined manually via a parameters (P) file. The atmosphere gas constant, surface pressure and surface temperature are also defined in the P-file. These values are used to calculate the surface density using the ideal gas equation. The density at each level is calculated from the surface upwards using the level temperature and hydrostatic theory. An infinite number of levels can be defined. However MLAM uses 32 atmosphere levels, which dictates the number of levels for this work as well. In A2D the atmospheric properties are the same all around the planet. This is unrealistic of course for trajectories over large distances. For the parachute descent phase this may be adequate. MLAM uses grid boxes of kilometre size in the horizontal directions. An EDL path can run over 1000 km in distance so eventually A2D will need to mirror this fact in its modelling of the atmosphere. A2D can simulate an entry vehicle, with detachable heat shield, parachutes and a lander with powered descent. The vehicle properties are defined in the same P-file as the atmosphere.

A2D was validated against Apollo era flight and simulation data rather than data from Mars landers because the Earth's atmosphere is less variable than Mars and its properties are well known. Figure 1 shows a comparison with simulation data from the Apollo era [11]. They ran several simulations to explore guided Apollo CM type trajectories. The altitude with time profile appears to be a good fit. There is a discrepancy of only 1.8 miles at the end of the EDL path. This is the order of error expected from A2D when run at a time step of 0.1 s. However Young and Smith [11] denote their results in units of nautical miles. If A2D results are converted into this unit then a discrepancy of well over 100 km exists. This result is not mirrored in the tightness A2D results follows the profile of altitude with time in the figure.

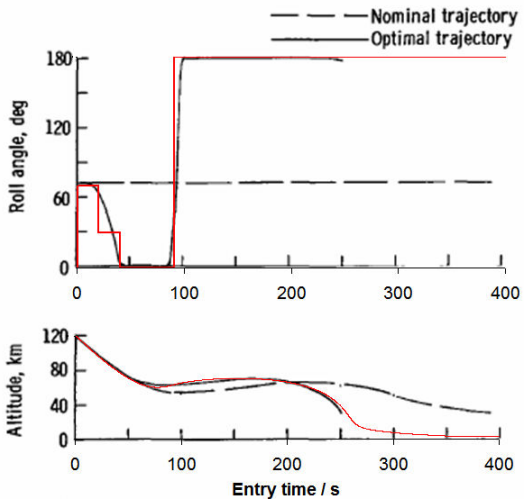

Fig. 1 Comparison with Apollo era simulations

Further validation of A2D, with reconstructed Best Estimate Trajectory (BET) data from the Apollo 6 mission, is shown in figure 2. While the match is reassuringly close there are noticeable deviations of A2D from the data. This is probably due to the approximate way A2D models the guidance computer roll commands and the fact that a real atmosphere will be different from the standard model.

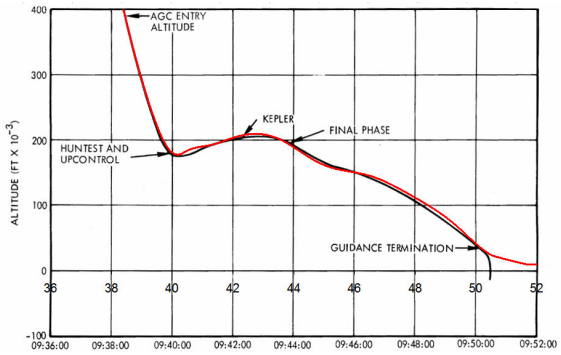

Fig. 2 Comparison with Apollo BET

4. A REALISTIC PILOTED MARS LANDER

This section describes the design of the piloted lander as used for the wind deflection tests in the next section. Surface area of the MTSV heat shield and parachutes are parameters required for these tests and so are investigated here. The mass has been defined in previous studies, e.g. see ref. [3].

There is a world-wide effort not only to develop our understanding of Mars through robotic missions but there are now programs to step towards human missions to that planet. Support of human exploration of Mars will certainly require landing heavier payloads than those already landed on Mars. It is not clear exactly how heavy these elements will be. Recent scenario studies such as NASA's Design Reference Missions Studies estimate several tens of tons of habitat and supporting equipment are required for surface missions of typically 1.5 years in duration [13]. To land these requires monster landers weighing perhaps over 30 tons. Studies suggest these may be extremely challenging to land. It may transpire that a smaller lander will suffice for a short term mission or perhaps smaller elements will be landed and assembled on the surface. It is reasonable to expect all these scenarios will require some degree of pin-point landing to make surface operations simple. In fact hypersonic guidance systems for Mars are being developed and will be demonstrated by future robotic missions.

The lander chosen for this study is a Mars Direct type vehicle whose design has the payload (habitat) sitting behind a large heat shield. Here we use the vehicle specified in reference [3] for the Mars for Less mission. The mission architecture requires the use of aerocapture to decelerate the Mars Transfer and Surface Vehicle (MTSV) into orbit around Mars before descending to the surface. To investigate the g level loading on the astronauts, determine the vehicle type (blunt or slender body) and the surface area of the heat shield a computer model of the habitat module with aeroshell was prototyped in A2D starting first with the aerocapture phase.

A spacecraft approaching Mars on a hyperbolic trajectory has to reduce its velocity enough so it enters into an orbit. With aerocapture this is done by passing through the atmosphere and using drag forces for deceleration. For crewed missions the deceleration must be kept below a certain level. A crew that has been in micro-gravity will suffer from muscle wastage, including the heart. For a deconditioned crew the maximum is between 3 and 5 g. Therefore it is important to fly the spacecraft along a path that minimizes the forces on the crew. The forces experienced by the crew will depend on the entry angle, the entry speed (which depends on the approach speed to Mars and the gravity of Mars), the desired target orbit (with a small eccentricity for large payload advantage of an all propulsive capture) and on the aerodynamic properties of the vehicle (specifically the lift over drag ratio). Implementing artificial gravity during the trip will help preserve the crew's physical strength for the descent and also for working on the surface and raising their g level tolerance during entry into the atmosphere. For this work it is assumed that the crew will be deconditioned, keeping this work within the bounds of reality as if returning from the ISS, for example.

To determine if a low lift blunt body type of vehicle could be used for aerocapture the dependence of corridor width on L/D was investigated. The calculation of the corridor widths also determined if the decelerations during aerocapture were low enough for a human crew. The vehicle used was an Apollo type blunt body heat shield with a L/D of 0.4. The mass was 46 mT and the effective area was 242 m^2 (C_D=1.242 and diameter=15.75 m). Three values of L/D were used. These were L/D=0 at an angle of attack of 0°, L/D=0.25 at an angle of attack of 25° and L/D=0.4 at an angle of attack of 40°.

This entry corridor width was determined using A2D. A vehicle with a fixed L/D was flown several times into the atmosphere of Mars from a start point (or entry point) of 125 km altitude and a start velocity of 7 km s^{-1} (which corresponds to a low energy transfer to Mars). The velocity vector angle or the entry angle (relative to the horizon) was varied until the vehicle was successfully captured into orbit. Then the entry

angle was decreased (more negative) until the vehicle experienced a peak deceleration of 5 g (limit for a deconditioned crew). This was then the undershoot angle. Once the undershoot entry angle had been established the entry angle was increased (less negative) until the vehicle was no longer captured into orbit and flew off into space. The g level never exceeded the limit so this was then the overshoot angle.

There was no accounting for uncertainties in navigation, atmosphere density or the aerodynamic properties of the vehicle during this process. An uncertainty of 0.4° in entry angle was assumed (from navigation, atmospheric and vehicle aerodynamic property uncertainties). This then makes the effective (safe) corridor 0.8° smaller than the actual corridor. The information can then be analysed to determine the best vehicle L/D value to use. The corridor for an L/D of 0 is only 0.2° which is too small to be certain of a successful aerocapture. The corridor widens with increased lift capability. An L/D of 0.25 opens up the corridor wide enough for a successful capture into orbit. To reach the target orbit (e=0.2) the vehicle has to reach the entry point at 10.7°. Therefore a blunt body design with an effective area of ~250 m^2 (as opposed to a slender body design) could be used for an aerocapture vehicle into Mars orbit. An L/D of 0.25 is well within the design heritage of Apollo blunt lifting body design. In fact L/D of up to 0.5 is possible with such a design. After the aerocapture phase into orbit comes the EDL phase.

It has been proposed [16] that a low L/D aeroshell (i.e. blunt body) together with an autonomous guidance algorithm and an accurate Inertial Measurement Unit (IMU) will reduce the error at parachute deployment to the navigation knowledge at IMU initialisation. It has been noted using Monte Carlo EDL simulations that for a blunt body the guidance program delivers the entry system right on target at parachute deployment in navigation space (the space in the lander's computer). However due to knowledge errors and IMU/Navigation error build-up the downrange error will be about 5 km and the cross range error will be about 1 km at parachute deployment. References [20] perform similar simulations for the MSL mission. They obtain a downrange delivery error of ±3 km. Presumably this error will be the same for a vehicle with a high L/D such as the biconic type vehicles used in NASA DRM 3.0 and other Reference Missions. IMU errors may be corrected by direct observations of the surface and comparing with maps. With aircraft, on Earth, IMU drift is corrected using GPS. In the literature high L/D biconic type vehicles are selected for their superior targeting ability but it is not clear to the authors how this is achieved. Indeed it is recommended that care be taken when designing in high L/D at the expense of an increased ballistic coefficient [16].

It has been suggested [20] that angle-of-attack modulation together with bank control, like the Space Shuttle, can help reduce the parachute deployment altitude uncertainty. With a blunt body the angle-of-attack can be controlled, in principle, via a movable mass. A biconic vehicle can use body flaps for both angle-of-attack and bank modulation. For a human scale biconic lander this may be a more practical approach, due to base architecture arguments (e.g. see reference [20]). However, here, we will stay with the blunt body approach as used with the Mars Direct type habitat. This is suitable for a scouting type missions to Mars.

The tried and tested EDL system for robotic landers has been to use a heat shield for thermal protection and aerobraking during the entry phase and then a parachute for braking to subsonic speeds were the final braking phase can be facilitated using retro rockets. The touchdown systems have differed though. The Vikings used semi-rigid legs while the rovers have used highly deformable airbags. For massive payloads airbags would be unrealistic. The next generation of NASA's Mars rover will touchdown on its wheels [14]. Staying as conservative as possible with the EDL design it is assumed here that the MTSV follows the design heritage of a heat shield for entry, parachute and retro rockets for descent and legs for landing.

The MTSV consists of four components that are assembled in Earth orbit before traveling to Mars. These are, from reference [3], the habitat, garage, lander and aeroshield (heat shield). They are assembled into a whole spacecraft in Earth orbit. Each component has its own set of properties such as mass, drag, lift etc. For a multi-component spacecraft there will be an effective centre where forces will act. Assuming the centre of mass for each component is located at its geometric centre the centre of mass of the assembled MTSV was calculated to be 5.38 m behind the centre of the heat shield.

It is essential for an entry capsule to maintain a forward facing heat shield for continuous thermal protection and for providing an effective drag surface. Stable flight can be achieved when the centre of mass is forward of the centre of pressure. Therefore it was desirable to identify the MTSV model properties so the centre of mass was in front of the centre of pressure. The effective surface area for the heat shield, normal to the z (long) axis was 242 m^2. The point where the drag acts on the shield was moved backwards by 10 m placing it 4.22 m behind the centre of mass of the MTSV. The centre of pressure was placed at this point where guided by flight tests in the Orbiter Space Flight Simulator [15]. Figure 3 shows a schematic diagram of the MTSV model derived from aerocapture flight tests in Orbiter. With an estimate of the centre of pressure it

is then possible to estimate the radius of curvature of the heat shield. From this information the heating rate during entry can be calculated to determine if such a shield can be used. It turns out the heating is not only very benign, it may be possible to use mass efficient inflatable technology as reported by reference [15].

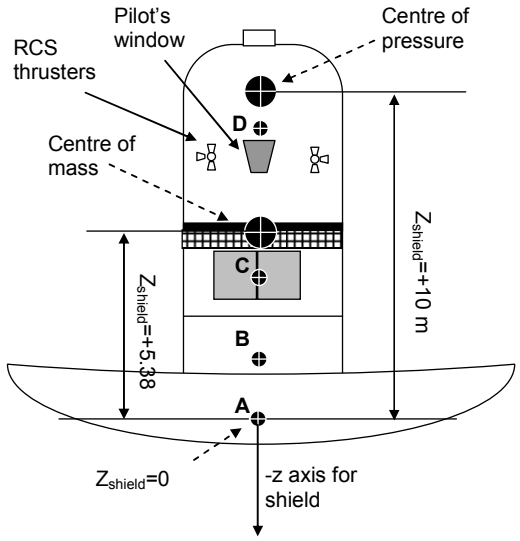

Fig.3 A piloted Mars lander

It has been reported by [16] that an all propulsive descent may be preferable to using parachutes. It is uncertain if larges parachute can be used. There may be stability problems and there may also be a significant time penalty when using large parachutes. This work aims to stay within the current design heritage of Mars landers and remain realistic as possible so useful conclusions for heavy robotic that may be flown in the near term can be provided. These landers will probably use parachutes before alternatives are developed.

To investigate parachute inflation times for a heavy lander like the MTSV a simple inflation simulation was conducted. This was used to find how exactly such a parachute can have a significant time penalty. The model assumed that the parachute inflated as a cylinder of constant height but with an expanding 'mouth' that is forced to open from air rushing in as shown in figure 4**.** The parachute was considered fully inflated when the radius of the cylinder was equal to the height of the cylinder, the broad shaped cylinder approximating the shape of a fully inflated parachute canopy.

The model was validated first by comparison with a skydiving type of parachute with a radius of 5 m and drag coefficient of 0.8. An inflation time of 3 s and a shock loading of 3 g were found. This compares favourably to a typical inflation time for a sports parachute which is between 2 and 3 seconds with a shock loading of 3-6g. A further comparison was made with results from POSTII a trajectory simulation program [17]. The parachute they modelled had a reference area of 178 m^2 which corresponds to a radius of 7.5 m assuming no gaps in the canopy. The drag coefficient for their parachute was 0.46. The payload used was a 761 kg Mars Lander and the atmosphere density at parachute deployment was 0.0135 kg m^3 (which corresponds to an altitude of 8.4 km in these simulations). The inflation time for the parachute modelled in reference [17] was 0.32 s and the drag on the parachute force was about 13 kN (or ~17 g). These numbers compare favourably with the author's own model results with an inflation time of 0.34 s and a maximum g level of just over 16 g.

It appears that a simple expanding cylinder model can approximate real parachute inflation dynamics. This model was then used to understand the dynamics of a large parachute on Mars as may be used by a piloted Mars lander. This of course ignored any engineering issues that may arise from deployment of such a large parachute. So for a parachute with a 30 m diameter an inflation time of 0.4 s was found and for a parachute with a 50 m diameter an inflation time of 0.8 s was found. This was travelling at Mach 3 at an altitude of 8 km. Exploring the relationship still further a 100 m diameter parachute inflation was simulated and found to take 1.3 s to inflate. Travelling at Mach 3 (~750 m s^{-1}) this means the distance travelled would be about ~1000 m during inflation. Including 10% porosity (to account for the loss of air through the gap in the top of the canopy) increases the inflation time by ~0.3 s giving a total inflation time of 1.6 s and distance travelled ~1200 m.

A piloted lander (50 mT) with a large heat shield (15 m) will decelerate to Mach 3 at an altitude between 10 and 15 km. Even using an extreme example of a 100 m diameter parachute it appears there will be plenty of time and distance for deployment. However at Mach 3 the g level on the crew will be about 20 g, possibly too high. The deceleration limit for an unconditioned crew is between 3 and 5 g during entry [18]. This is over periods of minute or so. A crew maybe able to tolerate higher g levels for short times such as during parachute deployment. However a shock loading of 20 g may still be very painful and even dangerous if the crew are not restrained properly.

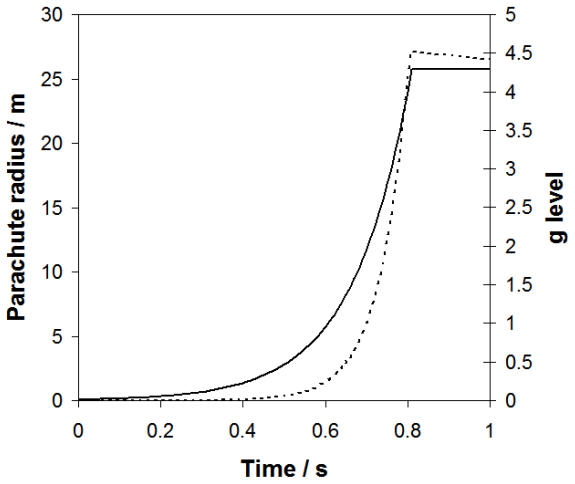

Fig. 4 Parachute inflation model

One way to reduce the g levels is to deploy the parachute at a lower altitude where the lander is travelling at a slower speed. EDL simulation suggests a 50 mT lander will reach 300 m s^{-1} (Mach 1.3) at 1.7 km. At this altitude parachute inflation of a 100 m diameter parachute will take about 5 s and the crew will experience only 5 g deceleration, which is a tolerable level. During parachute inflation the lander will then travel ~1.5 km downwards only leaving a second or so before hitting the ground. Obviously there is then a significant time penalty for deploying a large parachute close to the surface. However this does not mean such a parachute cannot be used at higher altitude (except the g levels will be high). A large parachute, say ~50 m in diameter, deployed at high altitude should be able to decelerate a 50 mT lander to subsonic speeds (and keep the g levels low) at several kilometres above the surface.

5. REALISTIC EDL SCENARIOS

MLAM surface and atmospheric data can be viewed by an earth science data graphics package called the Grid Analysis and Display System (GraDS) or the data can be exported to a text file. Here the temperature, wind speed, surface pressure and surface temperature at one particular location on Mars was exported into a parameters text file that was then read by A2D. The atmospheric density at the surface can then be calculated by A2D using the pressure and temperature at the surface together with the atomic mass of the atmosphere. For the rest of the atmosphere density can be calculated using the temperature data from MLAM, assuming an adiabatic atmosphere between levels. The calculation of the wind speed between levels was calculated assuming a linear interpolation. The gradient was defined by the distance between the levels divided by the difference of the wind speeds from those levels. The constant offset for that section was taken from the wind speed at the lower level.

Wind speed is output from MLAM as vector pairs, one south to north, labelled v, the other west to east, labelled u. The magnitude and direction of the wind can be calculated from these two vectors. Figure 5 shows the u component from the wind data at 0E 53S. The season was late autumn in the northern hemisphere or late spring in the southern hemisphere. The location is in the cratered uplands at an elevation of ~2 km above Martian "sea level". This location was chosen as it gave relatively high winds compared to other locations on the MLAM grid (-70W to 70E and -55S to 55N). This gives an upper limit to the magnitude of displacement experienced by a piloted lander. It is interesting to note that according to the water map derived by Mars Odyssey Gamma Ray Spectrometer this location is close to the boundary between high concentrations of water (towards the pole) and low concentrations of water (towards the equator) [19]. This makes an interesting landing site for exploration by humans although the EDLS design will be challenging due to the high elevation.

To asses the effect of Martian winds on a piloted lander the winds were applied in a normal direction to the trajectory. The drag area was calculated by assuming both the heat shield and parachute are hemispherical in form, using the side cross section area and assuming a drag coefficient of unity. This then gives an effective area of ~1000 m^2. The resulting displacement is shown in figure 5. During the entry phase the lander brakes using the drag surface of its 15 m diameter heat shield. The sideways acceleration on the lander from high altitude winds is only about 1 cm s^{-2}. An aero vehicle such as the blunt body entry configuration described in this work, with an L/D of 0.3 will surely have enough control authority to compensate for the tiny effect of these winds.

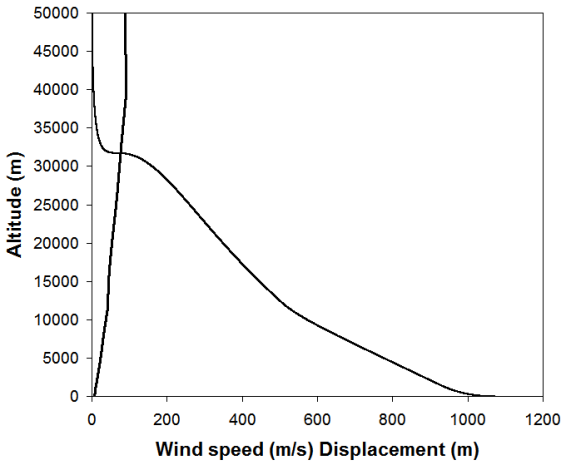

Fig. 5 Wind speed and lander side displacement

As can be seen in figure 6 there is a dramatic increase in sideways acceleration at an altitude of about 12 km.

This is due to the deployment of a large 50 m diameter parachute. This pushes the sideways velocity of the lander up to 6 m s^{-1} at touchdown. This is even though the surface speeds are only 4 m s^{-1}. This is an interesting result as it highlights that a high mass lander is hard to slow down i.e. resists slowing down once the winds drop down to a lower velocity value than the lander. In this example the winds drop below 6 m s^{-1} below an altitude of 50 m so there is not enough time for the sideways velocity of the lander to respond to the lower velocity winds. It is clear that it may not be safe to assume a lander will be moving to the side at the same velocity as the surface winds.

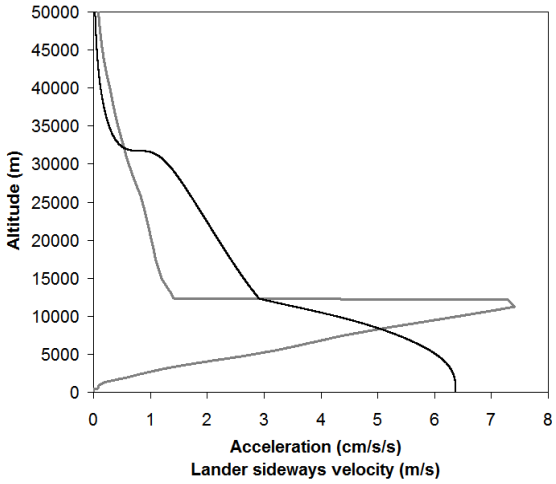

Fig. 6 Lander acceleration and sideways velocity

The sideways displacement was found to be about 1 km. Figure 5 was calculated assuming there is no correction during the hypersonic entry phase. Future robotic (and crewed) entry vehicles will have substantial control authority to overcome atmospheric uncertainties and so aid a pin-point landing [20]. So in reality the sideways displacement will be due to the parachute descent phase only. Once the parachute is released the power of the descent rockets can easily overcome any winds near the surface.

To investigate the lander displacement during descent by parachute an identical simulation was run but this time the winds are only engaged during the parachute phase. This results in a sideways displacement of ~300 m and a sideways velocity at touchdown of 4 m s^{-1}.

An additional EDLS design consideration that does not appear in the literature is consideration of how knowledge of the atmosphere may help manage risk. For example knowledge of the wind velocity profile with height could be used to calculate an optimal parachute release altitude for efficient use of fuel during the subsequent powered descent phase. To answer these questions the lander's EDL was run through A2D several times varying the parachute release height from 0 to 5 km.

First simulations were run without including rocket powered sideways adjustments for deflection by the winds. The MTSV just landed where it was blown. The retro rockets were started at such an altitude so the lander reached the target touchdown speed at zero altitude. It was found that keeping the parachute attached all the way to the surface was the most fuel efficient approach in this case. The amount of fuel used rapidly increased with higher parachute release altitudes. At lower release altitudes the rockets were already firing at parachute release but at higher altitudes the lander would free fall for some time before the rockets had to be started.

To account for wind drift and perform a pin-point landing an additional delta V had to be applied in the horizontal direction. This was during the powered descent phase, once the parachute was released. The longer the parachute was attached, the further the lander would be displaced and the more fuel used to fly to the landing site. However it was not the horizontal thrusting that ate up all the fuel. The lander was heavy enough and the Martian atmosphere was thin enough that once a delta V was applied horizontally the lander would coast in that direction. The fuel use becomes significant when the parachute was released near the surface because fuel was required for maintaining altitude over the surface i.e. hovering. This was large compared to the fuel required to correct for the sideways deflection by the wind. Conversely For very high parachute release altitudes the vertical delta V requirement for the powered descent phase increased so much that high fuel use was once again an issue.

There then must be an optimum release altitude for the parachute, where the ratio of fuel required for vertical delta Vs to horizontal delta Vs are not so large. The results from EDL simulations are shown in figure 7. The upper line shows the fuel remaining from tests without any sideways compensation and the lower line shows fuel remaining with compensation for wind displacement. The bottom line shows fuel use for a pin-point landing, where horizontal displacement by winds has been compensated for by the rocket engines, after parachute release. In this case the optimum release altitude for the parachute was found to be 2 km.

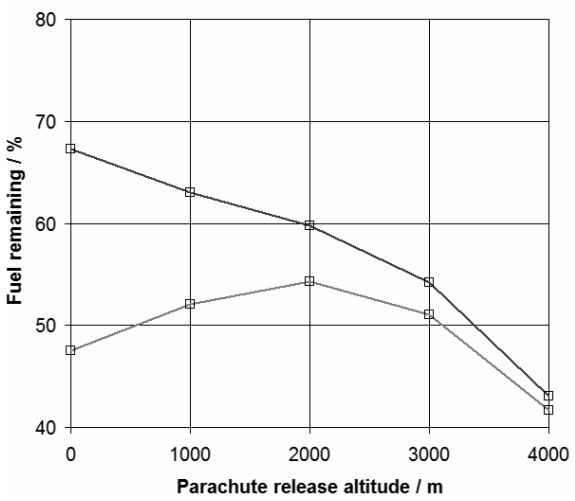

Fig. 7 Fuel use depending on parachute release

6. CONCLUSIONS

The parachute release altitude needs to be considered along with the timing of the powered descent phase to make efficient use of fuel and minimize risk. Online weather forecasting for Mars could help with this. Martian winds could be characterised to asses EDL designs for future landers on Mars. Atmospheric models like MLAM are realistic tools for tackling this task.

ACKNOWLEDGEMENTS

Many thanks to Janne Kauhanen for help exporting data from MLAM and answering numerous questions on computer modelling of the Martian atmosphere.

REFERENCES

1. Siili, T., Kauhanen, J., Harri, A-M, Schmidt, W., Järvenoja, S., Schmidt, W., Järvenoja, S., Read, P. L., Montabone, L. and Lewis, S. R., 2006, Simulations of atmospheric circulations for the Phoenix landing area and season-or-operation with the Mars Area Model (MLAM), Fourth International Conference on Mars Polar Science and Exploration, October 2-6, Davos, Switzerland, LPI Contribution No. 1372, p. 8049

2. Paton, M. D., 2005, Penetrometry of NEOs and other Solar System bodies, PhD thesis, the Open University, UK

3. Bonin, G., 2006, Reaching Mars for less: The reference mission design of the MarsDrive Consortium, 25th International Space Development Conference, Los Angeles

4. Bolling, L., 1968, Apollo 6 entry postflight analysis, Mission Planning and Analysis Section, NASA, Manned Spacecraft Center, Houston, Texas

5. Thermophysical GCM

6. Sanchez, B. V., Rowlands, D. D. and Haberle, R. M., 2006, Variations of Mars gravitational field based on the NASA/Ames general circulation model, Journal of Geophysical Research, v111

7. Rodin, A. V. and Wilson, R. J., 2006, Seasonal cycle of Martian climate: Experimental data and numerical simulation, Cosmic Research, v44, issue 4, pp. 329-333

8. Kauhanen, personal communication

9. Viking meteorological instruments

10. J. Balaram, R. Austin, P. Banerjee, T. Bentley, D. Henriquez, B. Martin, E. McMahon, G. Sohl, 2002, DSENDS – A high-fidelity dynamics and spacecraft simulator for entry, descent and surface landing, Jet Propulsion Laboratory, California Institute of Technology

11. Young, J. W. and Smith, R. E., Trajectory Optimization for an Apollo-Type Vehicle Under Entry Conditions Encountered During Lunar Return, Langley Research Center, 1968

12. Allouis, E., Ellery, A. and Welch, C. S., 2003, Parachutes and inflatable structures: parametric comparison of EDL systems: parametric comparison of EDL systems for the proposed Vanguard mission, Paper IAC-Q.3b.04, IAF Bremen

13. Drake, B. G. (Editor), 1998, Reference Mission 3.0 Addendum to the Human Exploration of Mars: The Reference Mission of the NASA Mars Exploration Study Team, Lyndon B. Johnson Space Center

14. Udomkesmalee, S. G. and Hayati, S. A., Mars Science Laboratory Focused Technology Program Overview, NASA tech publications, 2006

15. Irving, B., Sorley, A., Paton, M. and Bonin, G., 2006, Virtual prototyping of human Mars missions with the Orbiter space flight simulator, Mars Society Conference, Washington, DC

16. Braun, B. D., Wells, G. W., Lafleur, J. W., Verges, A. A. and Tiler, C. W., Entry, Descent and Landing Challenges of Human Mars Exploration, *29th AAS Guidance and Control Conference*, AAS 06-072, Breckenbridge CO, 2006.

17. Raiszadeh, B. and Queen, E. M., 2002, Partial validation of multibody program to optimize simulated trajectories II (POSTII) parachute simulation with interacting forces, Langley Research Center, Hampton, Virginia, NASA/TIM-2002-211634

18. Condon, G., Tiggs, M., Crus, M. I, Entry, Descent, Landing and Ascent, 1999, In J. Larson and L. K. Pranke (eds.) *Human Spaceflight: Mission Analysis and Design*, New York: McGraw-Hill, pp. 272-330

19. NASA/JPL, 2006, Water Map, http://mars.jpl.nasa.gov/odyssey/technology/grs.html

20. Wolf, A. A., Graves, C., Powell, R. and Johnson, W., 2004, Systems for pinpoint landing at Mars, AAS 04-272